J Fluoresc (2015) 25:341–353
DOI 10.1007/s10895-015-1516-2

ORIGINAL PAPER

# Spectroscopic and Quantum Mechanical Approach of Solvatochromic Immobilization: Modulation of Electronic Structure and Excited-State Properties of 1,8-Naphthalimide Derivative

**Soumya Sundar Mati · Sayantani Chall · Soumyadipta Rakshit · Subhash Chandra Bhattacharya**

Received: 20 August 2014 / Accepted: 20 January 2015 / Published online: 14 February 2015


**Abstract** Photophysical and spectroscopic properties of a fluorescent analogue, 2-(5-selenocyanato-pentyl)-6-chlorobenzo- [de]isoquinoline-1,3-dione (NP) in different solvents has been described in this paper using steady-state, time resolved spectroscopy and density functional theory (DFT) calculation. Stoke's shifted emission band in different solvents clearly demonstrate the highly polar character of the excited state, which is also supported by the enhancement of dipole moment of the molecule upon photoexcitation. Spectroscopic studies and multiple linear regression analysis method reveal that the solvatochromic behavior of the probe depends not only on the polarity of the medium but also on the hydrogen bonding interaction with the solvents. When the solvent effect was taken into account, the computed results show encouraging agreement with known experimental data. This article reveals the excellent correlation between the predicted and experimental spectral data of 1,8-naphthalimide derivative, providing a useful tool in the design of new fluorogenic probes having potential therapeutic activity.

**Keywords** Solvent effects · DFT calculations · Excited states · Simulated spectra · Lifetime

**Highlights**
- ✓ Solvent assisted tuning of photophysical properties of NP on the basis of steady-state and time resolved spectroscopy.
- ✓ Differential structural orientation in ground and excited states was interpreted by Density functional theory and configuration interaction singles.
- ✓ Similarity in computed infra-red (IR) and nuclear magnetic resonance (NMR) spectra with experimental findings.
- ✓ Knowhow of Nucleophilic or electrophilic reaction site of NP using electron density with molecular electrostatic potential surfaces.

**Electronic supplementary material** The online version of this article (doi:10.1007/s10895-015-1516-2) contains supplementary material, which is available to authorized users.

S. S. Mati · S. Chall · S. Rakshit · S. C. Bhattacharya (✉)
Department of Chemistry, Jadavpur University, Kolkata 700032, India
e-mail: sbjuchem@yahoo.com

S. C. Bhattacharya
e-mail: scbhattacharyya@chemistry.jdvu.ac.in

## Introduction

Optical characteristics of 1,8-naphthalimides, comprising an environment-sensitive special class of chromophores have aroused significant interest in research fields [1, 2]. Experimental findings along with theoretical calculations undoubtedly play an important role in naphthalimide derivatives for understanding detailed solvatochromic investigation [3, 4]. To date, research concerning these derivatives have explored several phenomena and consequently promoted their applications. However, concerted attenuates are being made in search of newly synthesized analogs in the light of steady state and time-resolved spectroscopy in association with DFT/TD-DFT and CIS/TD-DFT calculations.

1,8-naphthalimide derivatives have attracted the immense attention both for the intrinsic scientific challenges they pose and for their potential applications, particularly for the luminescence properties in visible light scope [5]. Being a luminophore compound, the photoinitiated processes of 1,8-

naphthalimides are of particular interest because of their widespread applications in biological and medical areas, as well as in supramolecular chemistry and materials science [6, 7]. They have fascinating properties to extend their use in tunable dye lasers [8], sensitizers for Grätzel solar cell [5], liquid-crystal displays [9], optical brighteners [6], to logic gate [1] and chemo-sensor [10]. Their versatility as probe for medical and biological purposes are also well-known for eg. DNA-cleaving agents [11], antitumor properties [4], potential HIV drugs [12] and fluorescent cell markers [9]. Very recently, Banerjee et al. [2] has shown the immense applicability of 1, 8-naphthalimides as DNA targeting binders, anticancer and fluorescent cellular imaging agents. As well, extensive researches revealing antitumor activity of 1,8-naphthalimides towards various human and murine cells have also been reported by Brana et al. [13]. Moreover, recent developments of these fluorescent derivatives as chemosensors further enhance and/or justify their acceptability [14, 15]. Accordingly fluorescence aided spectroscopy of 1,8-naphthalimide derivatives in homogeneous media is indispensable for various aspects of their colossal application. Solvent mediated spectroscopic studies of different 1,8-naphthalimides are going on till date [6, 16]. However, it is important to explore their photophysical characteristics experimentally as well as theoretically to enrich further the chemistry of these materials.

From this standpoint, the present work is intended to investigate the electronic properties of a photo-active 1,8-naphthalimide derivative employing both theory and experiment. We present here the spectroscopic properties of a biologically active selenocyanate substituted naphthalimide derivative (NP) (Scheme 1), which is expected to possess antioxidative property [17], in solvents of varying polarity. Our main objective is to investigate the solvent dependent radiative transitions and relaxation dynamics from the excited singlet state of this organoselenium compound. As well, theoretical calculations are also considered for more precise explanation of the experimental outcomes. Hence, in the present investigation, density functional theory (DFT) and configuration interaction singles (CIS) in association with time dependent-density functional theory (TD-DFT) methods have been used to investigate the absorption and emission spectra of NP in different solvents. However, the accuracy of the TD-DFT depends on the so-called adiabatic approximation [18–20], and approximate ground-state exchange correlation functional used in the DFT calculations [21]. In addition, the present theoretical study will provide structural and other basic properties such as conformational stability, vibrational frequency, NMR spectrum, total electron density, electrostatic potential and dipole moments of NP in various medium. Furthermore, the calculated results can be used as screening tools in developing new backbone and alternating group for the new chemical modification in experimental synthesis.

## Experimental Section

### Materials

Naphthalimide derivative, 2-(5-selenocyanato-pentyl)-6-chlorobenzo-[de]isoquinoline-1,3-dione was synthesized using the method [17] and it was purified by column chromatography. The compound was further vacuum-sublimed before use. The spectral grade solvents ethanol (EtOH), methanol (MeOH), acetonitrile (ACN), ethylene glycol (EG), glycerol (GLY), 1,4-dioxane (Diox), cyclohexane (Cyhx), n-heptane (n-Hept), dimethylformamide (DMF) were purchased from E. Merck, India. The solvents were dried according to the method described elsewhere [22] and used only after checking their purity fluorimetrically in the wavelength range of interest. Millipore water was used for preparation of the aqueous solutions.

### Methods

#### *Experimental*

The stock solution of compound NP (1.05 mM) was prepared in 1:1 dioxane-water mixture and a fixed amount of this concentrated solution was added to each experimental solution. A Shimadzu (model UV1700) UV–VIS spectrophotometer and

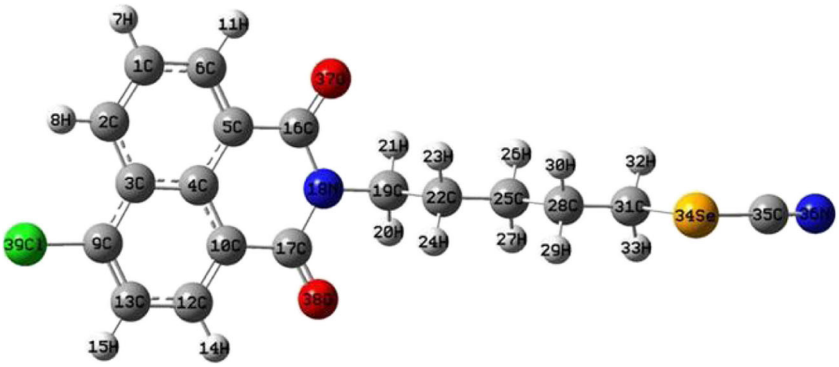


**Scheme 1** Structure of 2-(5-selenocyanato-pentyl)-6-chlorobenzo-[de]isoquinoline-1,3-dione (NP)

a Spex fluorolog-2 spectrofluorimeter with an external slit width of 2.5 mm were used to collect absorption and fluorescence spectra, respectively. All measurements were done repeatedly and reproducible results were obtained. All fluorescence spectra were corrected with respect to instrumental response. The fluorescence quantum yield ($\Phi_f$) was measured relative to standard probe quinine sulfate ($\Phi_f$=0.54 in 0.1 M $H_2SO_4$) [23]. Fluorescence lifetimes were determined from time-resolved intensity decay by the method of time correlated single-photon counting using a nanosecond diode LED at 370 nm (IBH) as light source. The data stored in a multichannel analyzer were routinely transferred to IBH DAS-6 decay analysis software. For all the lifetime measurements, the fluorescence decay curves were analyzed by single and bi-exponential iterative fitting program provided by IBH as in Eq. (1) [23]

$$F(t) = \sum_i a_i \exp\left(-\frac{t}{\tau_i}\right) \quad (1)$$

Where $a_i$ is the pre exponential factor representing the fractional contribution to the time resolved decay of the component with lifetime $\tau_i$. Average lifetime <τ>for bi-exponential decay was calculated using Eq. (2) [23]

$$\langle \tau \rangle = \frac{a_1\tau_1 + a_2\tau_2}{a_1 + a_2} \quad (2)$$

The FTIR spectrum of the powdered sample (using KBr pellets of the sample at a KBr–sample ratio of 100:1) was recorded with Perkin Elmer, Spectrum RXI equipment with a resolution of 2 $cm^{-1}$. The spectrum was recorded from 400 to 4000 $cm^{-1}$. $^1H$ spectra were obtained on a Bruker Avance DPX 300 spectrometer using $CDCl_3$ solution.

*Theoretical*

Prior to calculate excited state, ground state geometry of NP was optimized employing Density Functional Theory [24, 25] using the B3LYP [26, 27] functional with the standard basis set, 6-31G(d,p), for all atoms. All the structures correspond to global minima of the potential energy surface were confirmed by the vibrational frequency calculations. A variety of wave function-based methods such as, CASPT2, SAC-CI and CIS are the best choices to calculate the excited state geometry and optoelectronic properties [28]. A quite good number of studies [29, 30] have been performed using the above mentioned methods. The results obtained are comparable with the experimental results. Li et al. [31] had used DFT and CIS methods to optimize the ground- and excited-state geometry of Ethynylene Oligomers respectively and they calculated the absorption and emission spectra using the TD-DFT method with B3LYP exchange-correlation functional on the basis of these excited state geometries. To study the substituent effects of Indigo, Navarro et al. [32] also used DFT ground state structures and CIS excited structures with TD-DFT energies to determine absorption and fluorescence wavelengths respectively. So to get better results, we optimized the ground- and excited-state geometry of NP by DFT/6-31G(d,p) and CIS/6-31G(d,p) methods respectively. We then calculated the absorption and emission spectra of NP using the TD-DFT method [28, 33, 34] with B3LYP exchange-correlation functional. The results from theoretical calculations reproduced the trend as obtained from the experimental studies. All the ground- and excited-state optimization and spectral calculations have been carried out in different solvent medium using Tomasi's [35] polarized continuum model (PCM) in self-consistent reaction field (SCRF) theory in which the cavity is created via a series of overlapping spheres. In our theoretical calculations the dielectric constants 80.1, 32.7, 24.3, 37.5, 7.6, 2.02 and 1.9 were used to represent the water, methanol, ethanol, acetronitrile, tetrahydrofuran, cyclohexane and n-heptane solvent medium respectively. The entire simulations were performed using Gaussian 03 program [36] utilizing the $C_1$ symmetry.

## Results and Discussion

### Absorption and Emission

The UV–Vis absorption spectra of NP were recorded in various solvents of different polarity. The absorption spectra compiled in different nonpolar and polar solvents are shown in Fig. 1a and the corresponding spectral data are inserted in Table 1. The characteristic absorption maximum of NP has been observed to be shifted from 339 to 347 nm with variation of polarity from nonpolar to polar solvents. The absorption band in this region corresponds to л → л* transition (first excited singlet, $S_1$) of the molecule. With decreasing solvent polarity and proticity, it was found to have vibrational splitting of the absorption band at 346 nm. The vibrational splitting is prominent in n-hept and Cyhx. Interestingly, the л → л* absorption band is shifted to the red region and the vibrational band towards the blue with increasing solvent polarity. The red shift takes place in electronic transitions of the type л → л* with a higher dipole moment in the excited state $S_1$ than in the ground state $S_0$ [16]. High degree of coplanarity between the π system of the naphthalene ring and imide nitrogen invokes foremost contribution of electronic transition. The shift in magnitude of $\lambda_{max}^{abs}$ with the polarity of the medium suggests that the ground state of the molecule is polar. On excitation of the compound NP at the absorption maxima around 347 nm in the respective solvents, the emission spectra show a large red-shifted band in the region of 380–423 nm (Fig. 1b) from Cyhx

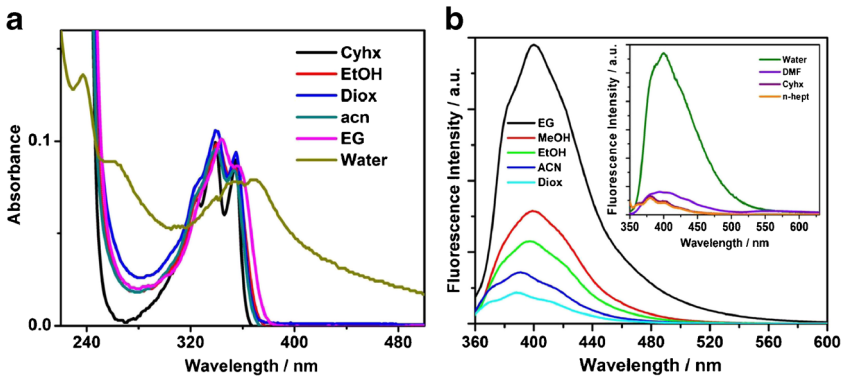


**Fig. 1** **a** Absorption ([NP]=$8\times10^{-6}$ M) and **b** emission profile of NP ($4\times10^{-6}$ M) in various homogeneous solvents. For emission spectra $\lambda_{excitation}$ corresponds to $\lambda_{max}^{abs}$ in respective solvents

to water. From results (Table 1), one can notice that the solvents exerted an evident influence on both the emission intensities and spectral maxima. The effect of the solvent polarity on the fluorescence maximum is more pronounced than that on the absorption maximum suggesting that the emitting state of NP is more polar compared to the ground state. Bathochromic shift in all solvents evinces progressively diminishing energy gap between the ground and excited states due to stabilization of excited state with increasing solvent polarity.

A plot of Stokes shift ($\Delta\bar{\nu}$ = difference between the transition energy corresponding to the absorption maxima E(A) and the fluorescence maxima E(F)) versus the microscopic solvent polarity parameter, $E_T(30)$ [37, 38] has been illustrated in Fig. 2a, where a linear correlation is obtained for NP. NP exhibits an overall increase of Stokes shift from nonpolar to polar solvent mainly due to the combined effect of both hydrogen bonding and polarity of the medium. Changing the medium from nonpolar to polar protic, stabilizes the excited state of NP which causes red shift and consequently stokes shift increases.

**Table 1** Absorption and emission wavelength maxima ($\lambda_{max}$), Quantum yield ($\Phi_f$) and Stokes shift ($\Delta\bar{\nu}$) of NP in different homogeneous media and solvent polarity parameter ($E_T(30)$)

| Solvent | $\lambda_{max}^{abs}$ (nm) | $\lambda_{max}^{emis}$ (nm) | $\Phi_f$ | $\Delta\bar{\nu}$ ($cm^{-1}$) | $E_T(30)$ (kcal $mol^{-1}$) |
|---|---|---|---|---|---|
| Water | 347 | 405 | 0.080 | 4127.1 | 63.1 |
| EG | 343 | 400 | 0.406 | 4154.5 | 56.3 |
| MeOH | 341 | 399 | 0.130 | 4262.9 | 55.5 |
| EtOH | 341 | 397 | 0.098 | 4136.6 | 51.9 |
| ACN | 340 | 390 | 0.058 | 3770.7 | 46.0 |
| DMF | 340 | 393 | 0.011 | 3966.5 | 43.9 |
| Diox | 340 | 388 | 0.038 | 3638.6 | 36.3 |
| Cyhx | 339 | 380 | 0.006 | 3182.7 | 31.2 |
| n-Hept | 339 | 380 | 0.005 | 3182.7 | 31.1 |

To investigate the influence of solvent upon solvent–fluorophore interactions, the fluorescence emission was recorded at different percentage composition of water-Diox mixture (Figure S1). In Diox-water mixture, with increasing water content, the fluorescence intensity enhances with red shift. Interestingly water addition above 80% to the mixture causes decrease in intensity to some extent. The combined effect of hydrogen bonding and polarity of the medium are the responsible factors for such kind of emission behavior of NP. Presence of carbonyl oxygen and imide nitrogen allows efficient intermolecular hydrogen bonding interaction with solvent molecules. So the progressive decrement of fluorescence intensity with a red shift in emission maximum on gradual water addition to the mixture possibly due to a modification of intermolecular hydrogen bonding interactions between water and the probe molecule by the hydrogen bonded network present in water [39]. As more and more water molecules replace the dioxane molecules around NP, the microenvironment around NP consists of mainly associated water cluster of hydrogen bonding network.

It is interesting to know the changes in fluorescence quantum yield ($\Phi_f$) of NP in different solvents. The variation of $\Phi_f$ values (Table 1) with solvent polarity parameter $E_T(30)$ is plotted in Fig. 2b where a linear correlation of $\Phi_f$ with solvent polarity of different homogeneous solvents except EG has been observed. Dey et al. [40] and Ye et al. [41] ascertained that the highly viscous medium was responsible for increasing quantum yield and lifetime of a probe. Hence also for NP, viscosity plays a major role for high quantum yield of NP in EG medium.

## Multiple Linear Regression Analysis

The solvent effects were exploited to determine the physical and chemical interaction by NP using empirical solvents parameters. Kamlet-Taft [42] solvatochromic comparison method was used for elucidating and quantifying this solute-solvent interaction. According to this method absorption [E(A)] and emission [E(F)] band energies (kcal/mol) can be

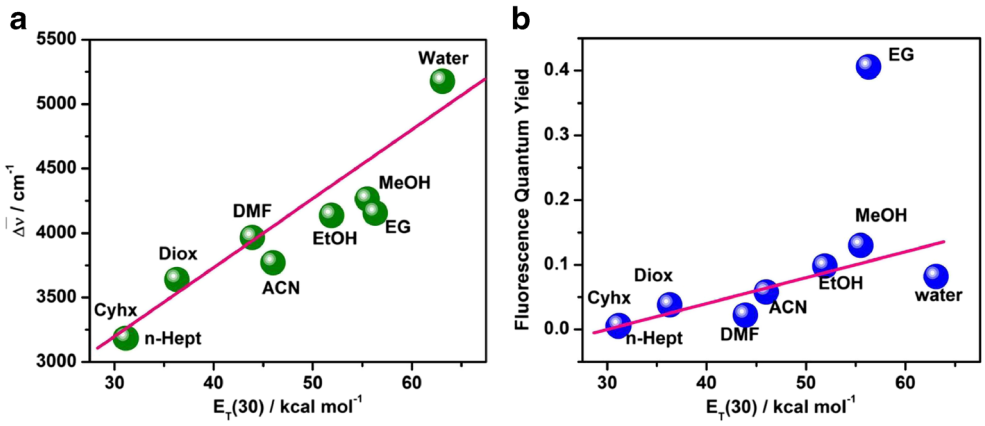


**Fig. 2** **a** Variation of Stokes shift of NP as a function of solvent polarity parameter ($E_T(30)$). **b** Plot of quantum yield versus $E_T(30)$ for different solvents

correlated using the multiple linear regression analysis approach of Abraham et al. [43] as shown below in Eq. (3)

$$E = E_0 + A\alpha + B\beta + C\pi^* + \cdots \quad (3)$$

Where $E_0$ is the value of E in a hypothetical inert solvent. Taft's solvent parameter $\pi^*$ value is an index of the solvent dipolarity/polarizability and $\alpha$ and $\beta$ values [42] represent the hydrogen bond donating or electron pair accepting and hydrogen bond accepting or electron pair donating ability of the solvent, respectively. A, B and C are the contribution of the polarity parameters $\alpha$, $\beta$ and $\pi^*$ respectively to the spectral shifts. The values obtained here:

$$E(A) = 84.74 - 0.73\alpha + 0.97\beta - 0.97\pi^* + \cdots \quad (4)$$

$$E(F) = 75.61 - 1.13\alpha - 3.23\beta - 0.36\pi^* + \cdots \quad (5)$$

The different parameters from absorption and emission energy show that in its excited state, NP interacts with its environment differently than its ground state. From E(F) value it is apparent that H-bond accepting parameter ($\beta$) of solvent plays a major role in excited state. The ratios of coefficient of $\beta$ over $\alpha$ and $\pi^*$ in excited state are B/A=2.85 and B/C=8.97. This clearly implies the dominance of H-bond acceptance ability over H-bond donation ability and dipolarity/polarizability of the solvents. The bathocromic shift in absorption and emission maxima can also be explained from the negative value of C i.e. coefficient of dipolarity/polarizability of solvents.

## Time Resolved Fluorescence Study

Fluorescence lifetime measurement often serves as a sensitive indicator of the local environment of a fluorophore to characterize the spectral properties and dynamics in the excited state [23, 39, 44]. Representative time-resolved decay profiles of NP in various solvents are displayed in Fig. 3 and the relevant data are summarized in Table 2. To delve into the photophysics of the drug in homogeneous environment, the lifetime of the species formed in the excited state was assayed by monitoring the emission at its corresponding steady-state emission wavelengths. All the decays of NP are bi-exponential irrespective of the solvent polarity with a $\chi^2$ value near unity. The biexponential fitting does not necessarily indicate that the decay curve has only two discrete time constants; rather, it may imply a distribution of time constants around two well-separated values. Using two other probes Dhar et al. [39, 45] speculated such type of biexponential decay in various solvents as the compounds experienced two different local conformations with the solvents. Gan et al. [46] and Poteau et al. [47] also clarified biexponential decay of the probes in solvents using PET mechanism. Alternatively, in Pradhan's [48] report, the biexponential decay was explained on the basis of solvent reorganization and collisional deactivation with the solvents molecules. So in case of NP we may conjecture the biexponential decay of NP in different solvents due to two different local environments experienced by the probe. Increase in the polarity of the solvent leads to an augmentation of lifetime except ethylene glycol and DMF. The

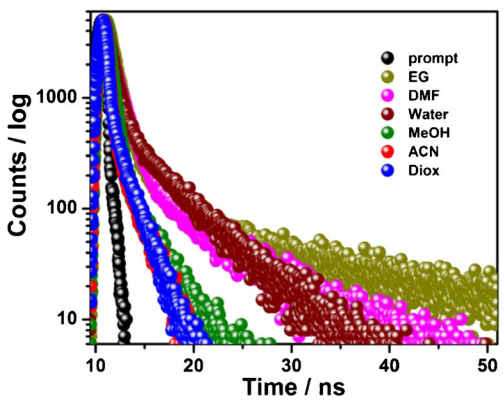


**Fig. 3** Time-resolved decay profile of the NP molecule in different solvents at room temperature monitoring at the corresponding $\lambda_{max}^{emis}$

**Table 2** Fluorescence lifetimes (τ), fractional contribution in excited state ($a_1$and $a_2$), average lifetime of NP in different solvents

| Solvent | $a_1(a_2)$ | Lifetime, $\tau_1$ (ns) | Lifetime, $\tau_2$ (ns) | $\tau_{avg}$ | $\chi^2$ |
|---|---|---|---|---|---|
| Water | 0.66(0.34) | 0.92 | 5.85 | 2.60 | 1.14 |
| EG | 0.82(0.18) | 1.05 | 8.88 | 2.46 | 1.15 |
| MeOH | 0.88(0.12) | 0.59 | 3.27 | 0.91 | 1.00 |
| EtOH | 0.88(0.12) | 0.52 | 2.81 | 0.79 | 1.04 |
| ACN | 0.79(0.21) | 0.25 | 2.00 | 0.62 | 0.95 |
| DMF | 0.81(0.19) | 1.24 | 8.25 | 2.57 | 1.29 |
| Diox | 0.73(0.27) | 0.29 | 1.94 | 0.74 | 1.04 |
| Cyhx | 0.73(0.27) | 0.33 | 1.17 | 0.56 | 1.28 |
| n-Hept | 0.65(0.35) | 0.18 | 0.70 | 0.36 | 1.05 |

effect of polarity on fluorescence lifetime is same as the fluorescence quantum yield. In case of ethylene glycol the decay time is higher which is due to the increase in viscosity of media. However in DMF the probe shows a higher life time value, which may be due to enhanced stability as a result of electron transfer from the electron rich DMF to the electron deficient center of probe [49].

## Excited State Dipole Moment

In general, a method of estimation of change in dipole moment of the probe upon excitation was obtained from solvatochromic data assuming a dielectric continuum description of the solvent [44]. The extent of charge separation on electronic excitation of NP was determined by measuring the change in the dipole moment utilizing the Stokes shifts ($\Delta\overline{\nu}$) and a solvent parameter which is a function of both dielectric constant and refractive index of the solvents. According to Lippert–Mataga equation [23] (Eq. (6))

$$\Delta\overline{\nu} = \frac{2\left(\mu_e - \mu_g\right)^2}{hca^3}\left[\frac{\varepsilon-1}{2\varepsilon+1} - \frac{n^2-1}{2n^2+1}\right] + \text{const} \qquad (6)$$

Where ‘a’ is the Onsagar cavity radius swept out by the fluorophore, ε and ‘n’ are the dielectric constant and refractive index of the solvent respectively. $\Delta\mu=\mu_e-\mu_g$ is the difference between the excited state ($\mu_e$) and ground state ($\mu_g$) dipole moments of the probe. Plot of $\Delta\overline{\nu}$ against Δf for NP (Figure S2) results Δμ from the slope, where

$$\Delta f = \frac{\varepsilon-1}{2\varepsilon+1} - \frac{n^2-1}{2n^2+1}$$

Except in water the correlation between $\Delta\overline{\nu}$ and Δf is linear. However the present behavior could be rationalized by solvent stabilization of NP due to several effects: dipole-dipole interactions, hydrogen bonding and dipole-induced dipole interactions. In water the increasing polarity stabilizes the NP through hydrogen bonding. Using DFT, the longest distance between the carbonyl oxygen (37O) and chlorine (39Cl) at the naphthalimide ring as the Onsager cavity radius (3.79 Å) has been calculated. From the slope of Eq. (6) the dipole moment change on excitation is estimated to be 3.99D for NP. On excitation from the ground to excited state the enhanced dipole moment of NP further emphasizes the increase in polarity of the emissive state causing the red-shift of the emission maxima with polar solvent.

The dipole moment of NP in different medium using B3LYP/6-31G(d,p) level of theory is summarized in Table S1. In water the dipole moment of NP is 9.62D (GS) and in excited state it changes to 10.96D at B3LYP/6-31G(d,p) method whereas in similar condition the dipole moments in n-Hept are 8.82D and 9.42D respectively. It is worth noting that not only the excitation but polarity also significantly increases the dipole moment value of NP which may be due to the dielectric relaxation of the solvents [50].

## Theoretical Calculations

### *Ground and Excited-State Geometry Optimization*

The optimized structures of the ground ($S_0$) and excited state ($S_1$) of NP in various solvents, calculated employing the DFT and CIS method respectively, are depicted in Fig. 4. It is noticed that the geometrical parameters like bond lengths and dihedral angles of NP are affected upon excitation from ground state to excited state. As optimization steps proceed, modification of such geometrical parameters associated with optimization energy and RMS gradient on going from ground to excited state are displayed in Figure S3. Among different solvents, there are also some modifications of the molecular geometry employing the continuum solvation model. The optimized excited state structure was compared with the ground-state structure of NP and comparisons of bond lengths and bond angles between the excited and ground state of NP in different solvents are depicted in Table S2. The average root mean square deviation (rmsd) between the internal coordinates [28, 51] obtained from the studied structure using DFT and CIS methods is 0.02Å. Moreover, the resulting structure, depicted in Fig. 4, is planar with the exception of the alkyl group, which is tilted out-of-plane with the angle 16C-18N-19C-22C. The structure of NP molecule in CIS method is considerably different from DFT method so that the value of central dihedral angle (16C-18N-19C-22C) between naphthalimide ring and alkyl moiety is reduced from 89.52 to 89.09° in water and 89.67 to 88.85° in Cyhx. The calculated dihedral angles of 12C-10C-17C-38O are 179.20 and 179.33° for water and n-Hept, respectively in the CIS excited state.

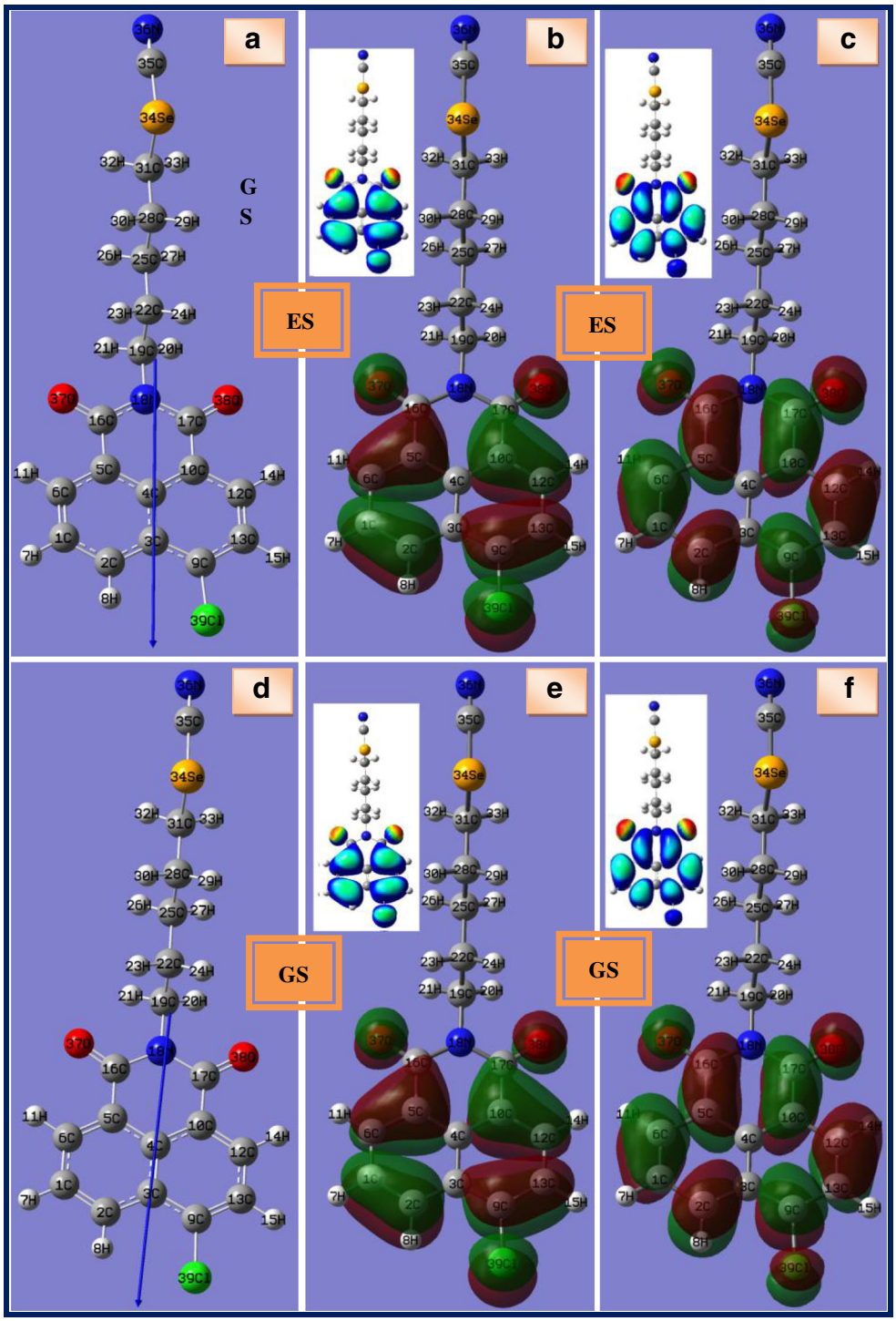


**Fig. 4** Optimized **a** ground and **d** excited state structure of NP molecule in water. The *arrows* show the direction of dipole moment vector. The density plot of the highest occupied molecular orbital (HOMO) and the lowest unoccupied molecular orbital (LUMO) of **b** GS HOMO **c** GS LUMO **e** ES HOMO **f** ES LUMO. Inset:3D ESP-SCF plot on MO surface of corresponding MO-diagram having scale −5.0e-2 to 5.0e-2

This suggests that the conjugated geometry of NP possess more planar orientation in aqueous medium compared to n-Hept in their CIS excited state and consequently it is observed that in comparison to n-Hept the fluorescence intensity is higher in water. The bond length 10C-17C is also shortened in excited state from its typical standard value of 1.46 Å indicating the double bond property of the bond.

*Simulated Absorption Spectra*

According to the vertical electron transition mechanism in the absorption process, the optimized ground state (GS) geometry is kept, while TD-DFT calculation of the optimized ground state yielded information on the character of the ground state as well as the transition energy and oscillator strength (f),

**Table 3** Calculated Absorption and Emission wavelength maxima, Frontier Molecular Orbital Energy along with Oscillator strength of NP molecule in ground and excited state in different solvents

| | Absorption maxima (nm) | Emission maxima (nm) | Oscillator Strength | | HOMO (eV) | | LUMO (eV) | |
|---|---|---|---|---|---|---|---|---|
| | | | GS | ES | GS | ES | GS | ES |
| Water | 348 | 386 | 0.32(H→L) | 0.31(H→L) | −6.48 | −6.21 | −2.57 | −2.72 |
| MeOH | 348 | 385 | 0.31(H→L) | 0.32(H→L) | −6.49 | −6.33 | −2.57 | −2.84 |
| EtOH | 348 | 385 | 0.32(H→L) | 0.32(H→L) | −6.49 | −6.33 | −2.57 | −2.84 |
| ACN | 347 | 384 | 0.32(H→L) | 0.32(H→L) | −6.49 | −6.33 | −2.57 | −2.84 |
| Cyhx | 346 | 383 | 0.32(H→L) | 0.32(H→L) | −6.62 | −6.46 | −2.69 | −2.95 |
| n-Hept | 345 | 383 | 0.31(H→L) | 0.32(H→L) | −6.63 | −6.46 | −2.69 | −2.95 |

which is related to the absorption spectrum of NP. Using polarizable continuum model (PCM), the theoretical absorption spectrum of NP in different solvent medium is performed and corresponding data are listed in Table 3. The interesting trend on oscillator strength values in the table shows that $S_0 \rightarrow S_1$ transition have the largest value in all inspected solvents. As $S_0 \rightarrow S_1$ transition plays the major contribution in the absorption spectrum, the TD-DFT method gives a good interpretive transition to the promotion of an electron from HOMO to LUMO. The theoretical absorption spectrum of NP exhibits single band centered at around 347 nm which corresponds to л → л* transition in different solvents.

In general, the absorption spectra calculated using the TD-DFT method is in accord with the values reported in experimental studies. The maximum of absorption in the simulated spectra is located between 3.568 and 3.587 eV in different solvents, which is in good agreement with the experimental data presented in Table 1. In corroboration to the experimental absorption maxima, the calculated absorption maxima also exhibit a red-shift of about 3 nm from n-hept to water. The calculated $\lambda_{max}^{abs}$ values of NP are in well agreement with experimental results, with the negligible deviations of 0.060 eV (±0.009). Thus, this result acclaims to the computational approach. As the TD-DFT method is more advantageous and the data from TD-DFT coincides with experimental values, so appropriate electronic transition energies can be predicted at these levels for this kind of system [9].

### *Simulated Emission Spectra*

To explore the emissive properties, the geometry optimization of the excited state (ES) in CIS method and TD-DFT calculation were carried out to get subsequent information regarding the transition energy and oscillator strength, which are related to the emission spectra of NP. The structural parameters obtained with the TDDFT-B3LYP and CIS methods are similar. Along with the available experimental results (Table 1), the calculated absorption and emission spectra of NP and corresponding oscillator strength in different solvents are summarized in Table 3 in which the fluorescence wavelengths show similar tendency with the absorption wavelengths ($\lambda_{max}^{abs}$). For the emission spectrum the difference between TDDFT/CIS calculated data and experimental data is only 0.072 eV (±0.03) and the comparisons of spectral nature of experimental and simulated ones are depicted in Fig. 5. As seen in Fig. 5, the calculated and measured values of absorption and emission wavelength maximum are in good agreement. This agreement lends credence to the density function calculations and the assumptions that were made to determine the solvent effects on NP. Meanwhile, the oscillator strength is quite appreciable also. Using CIS/TDDFT method the calculated emission spectrum of NP exhibits single band centered at around 385 nm which corresponds to $S_1 \rightarrow S_0$ transition for different solvents. However, the general trends of bathochromic emission wavelength shift for calculated spectra of NP in different solvents are the same and do not show significant deviation compared to experimental results. Among the six different solvents the emission wavelength of the compound is red shifted about 3 nm from n-Hept ($\lambda_{max}^{emis}$ = 383 nm) to water ($\lambda_{max}^{emis}$ = 386 nm). Hence, the solvent phase calculation of fluorescence wavelengths using TD-DFT method is suitable for the agreement with experimental findings of this fluorophore.

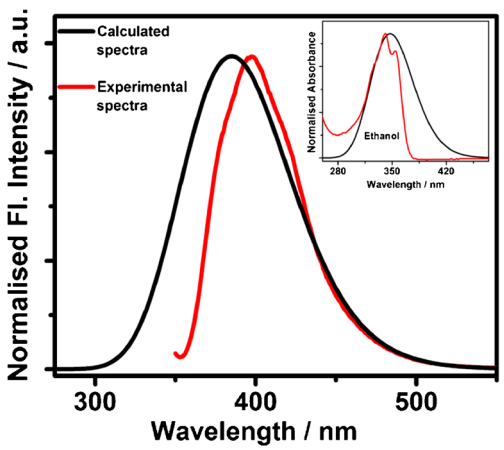


**Fig. 5** Comparison of calculated and experimental emission spectra of NP in ethanol. *Inset* shows the same for excitation spectra

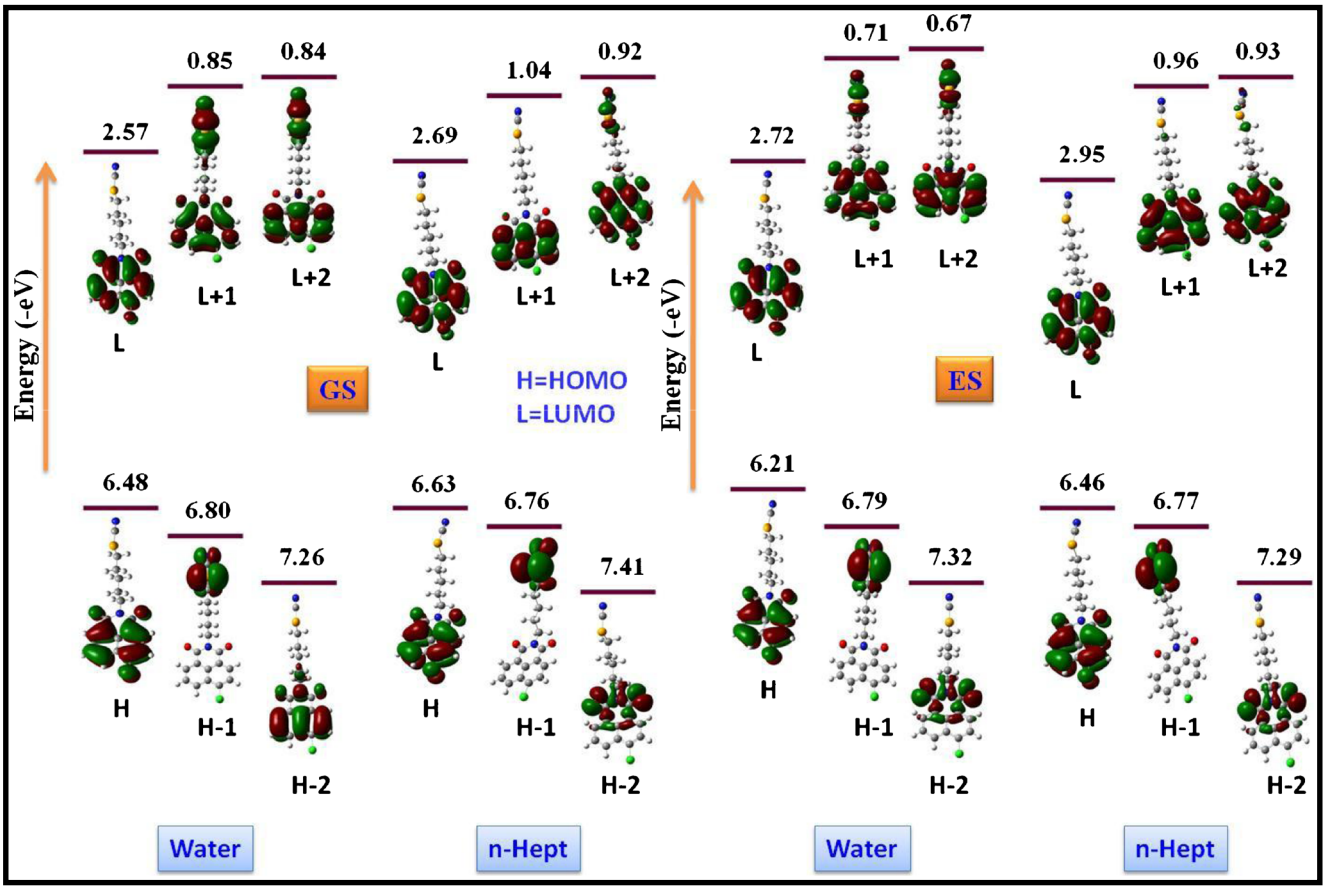


**Fig. 6** Contour plots and energies of frontier orbitals (HOMO, H-1, H-2 and LUMO, L+1, L+2) corresponding GS and ES for NP in water and n-Hept

*Frontier Molecular Orbital*

The highest occupied molecular orbitals (HOMO) and the lowest unoccupied molecular orbitals (LUMO) can provide a reasonable qualitative indication of the detailed electronic properties. In view of their ability on electron or hole transport in feature of electron density contour, the energy levels of the frontier molecular orbitals especially HOMO and LUMO as well as their spatial distributions are crucial parameters for determining the optoelectronic properties [28, 52]. Figure S4 presents the density plot of HOMO and LUMO orbitals of NP in ground and excited state (aqueous phase) as well as the corresponding energy values in solvents of different polarity are also tabulated in Table 3. The molecular orbital diagrams of NP are plotted with the isovalue of 0.02. From the close look of orbital plots the molecule have the typical $\pi$ molecular orbital characteristics which are somewhat altered by the solvent change. Concerning the spatial distribution of the molecular orbitals, we found that HOMO is delocalized over the bonding orbitals between 1C and 2C; 6C, 5C and 16C; 9C and 13C; 12C, 10C and 17C; 37O; 38O; 39Cl whereas the LUMO orbital is characterized with bonding orbitals between 1C and 6C; 2C; 9C; 12C and 13C; 10C and 17C; 5C and 16C; 37O; 38O; 39Cl. Consequently, Fig. 6 illustrates that, for all inspected solvents, both HOMO and LUMO in their ground and excited states are fully delocalized over the naphthalimide ring, but on introduction of H-1 and L+1, H-1 is confined in the selenocyanate moiety of NP, whereas L+1 becomes delocalized throughout the molecule. It is worth mentioning here that the molecular orbital lobes which located on the oxygen atoms of the HOMO and LUMO surfaces is a non-bonding orbital. Hence, the electrons in oxygen atom act like a lone pair of electrons in a Lewis structure. Except in water

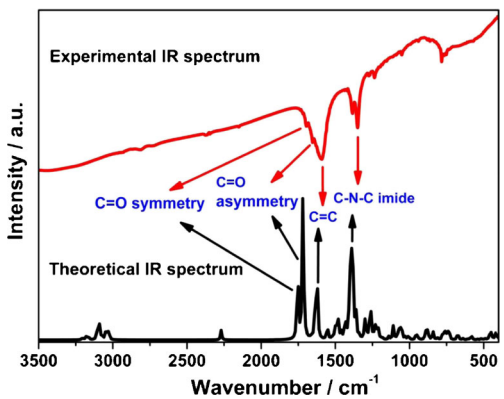


**Fig. 7** Simulated and experimentally observed Infra Red spectra of the compound

(GS), the molecular orbital lobes of NP spreading over the H-2 surfaces of naphthalene moiety are of antibonding character because it has a node between adjacent nuclei with lobes of opposite sign (Fig. 6) and in GS water antibonding character is only on the -$(CO)_2$ imide- moiety. p-orbital on the oxygen atom of -$(CO)_2$ imide- moiety of NP is a major contributor of H-2 surfaces whereas in water (GS) major contributor is for $\pi$ orbital of naphthalene ring. The excitation (at 348 nm) of complex occurs with oscillator strength of 0.32 and is composed of the transition from HOMO to LUMO in the ground state MOs. Besides, the transition between HOMO to LUMO having oscillator strength 0.31, produces a fluorescent band at 386 nm among the excited state MOs in water.

To gain insight into the effect of polarity on FMO, the energy difference between HOMO and LUMO of NP were examined in different solvents. Both HOMO and LUMO

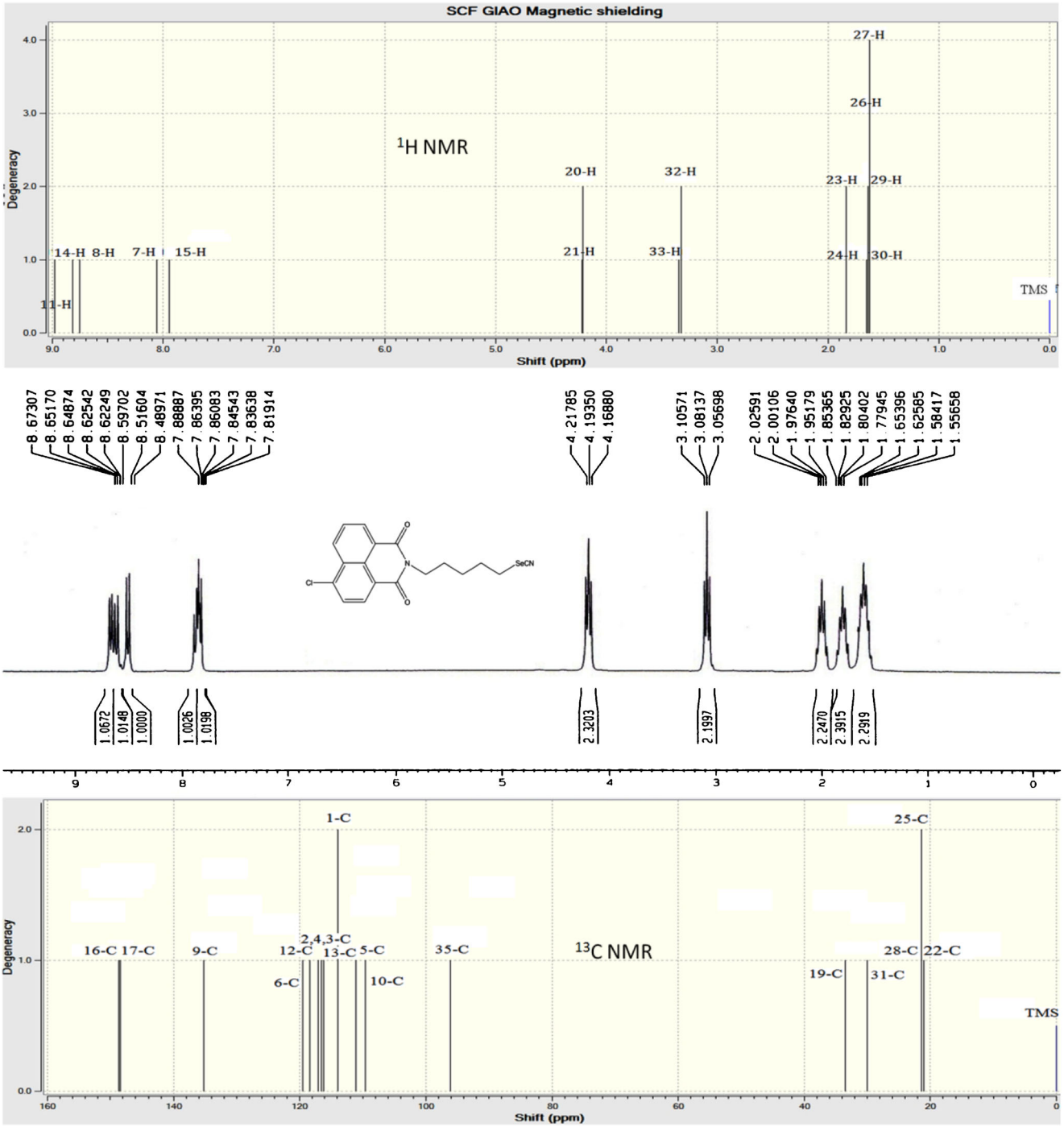


**Fig. 8** Simulated and experimentally NMR spectra of the title compound

levels lower down as the solvent polarity rises. However, for the excitation process the largest HOMO–LUMO gap is 3.93 eV for n-Hept and it continuously decreases to 3.91 eV (water). The situation is now analogous for the fluorescence emission where the HOMO–LUMO gap shrinks on going up solvent polarity. Among the solvents, n-Hept has a maximum H-L energy gap of 3.51 eV and water has a minimum H-L gap of 3.48 eV whereas an intermediate H-L gap of NP belongs to the solvent ACN (3.49 eV). As expected, the molecules with a small H-L energy gap possess maximum absorption and emission wavelength [28]. However, to gain the maximum stability from n-Hept to water, the energy of Frontier Molecular Orbitals of NP changes according to the solvent polarity. Our quantum chemical analysis regarding the H-L energy gap shows that both emission and absorption spectral maxima are red shifted in water relative to nonpolar solvents.

*IR and NMR*

We have calculated the vibrational spectra of NP using B3LYP method (scaling factor 0.96) with 6-31G(d,p) basis set and then this result is compared with experimental results (Fig. 7). According to Grabchev et al. [53] CNC (imide) peak is the characteristic for naphthalimide molecule. The characteristic vibrational peak for CNC (imide) of NP is assigned to at 1360 $cm^{-1}$ (experimental) and 1388 $cm^{-1}$ (calculated). The other two peaks for C=O (symmetry) and C=O (asymmetry) also show good agreement with experimental values (1700 $cm^{-1}$, 1650 $cm^{-1}$) and calculated ones (1750 and 1710 $cm^{-1}$). The C=C bond is also prominent for both the calculated (1618 $cm^{-1}$) and experimental (1590 $cm^{-1}$) spectra but in experiment the latter three peaks are combined to a broad spectrum but individual peaks.

The experimental and theoretical chemical shift values for $^{1}H$ NMR (Table S1) of NP and corresponding spectra are given in Fig. 8. The theoretical chemical shift values were calculated by DFT/B3LYP methods using 6-31G(d,p) basis set. Tetramethylsilane (TMS) was taken as reference compound for the calculation of $^{1}H$ and $^{13}C$ NMR chemical shift and it was also optimized at the same level of theory. $^{13}C$ NMR values are also shown in Fig. 8. In general, highly shielded $^{1}H$ protons appear downfield and vice versa. Experimental peaks (exp) obtained at 8.66(dd), 8.61(dd), 8.50(d), 7.86(t) and 7.83(d) ppm are due to the aromatic hydrogens and consequently for simulated peaks (smp) corresponding δ values are 8.97(11H), 8.75(8H), 8.81(14H), 8.05(7H) and 7.94(15H) ppm. Alkyl hydrogens (20H and 21H) attached with electronegative nitrogen atom of naphthalimide moiety are more deshielded and peaks appear at more higher chemical shift values 4.19(t) (exp) and 4.21 (smp) ppm. Similarly the 32H and 33H peaks at 3.08(t) (exp) and 3.32 (smp) ppm are due to tie with Se atom. Other alkyl hydrogens (29H and 30H; 26H and 27H; 23H and 24H) show the δ values 1.58(q), 1.82(q), 2.0(q) (exp) ppm and 1.62, 1.66, 1.80 (smp) ppm respectively. The predicted $^{1}H$ chemical shift values of DFT were in closer agreement with the experimental values for all of the protons of NP.

## Conclusion

Herein we have attempted to summarize a strategy to tune the solvent dependent electronic properties of NP based on the results of calculated and experimental spectroscopy. Spectroscopic studies reveal that the solvatochromic behavior of NP depends not only on the polarity of the medium but also on the hydrogen bonding properties of the solvents. A Kamlet– Taft analysis shows that in the excited state, NP forms a stable hydrogen bond complex with solvents having high hydrogen bond acceptance abilities and low hydrogen bond donor character. The DFT and CIS calculations were used to investigate the absorption and emission spectra of NP in the framework of TD-DFT and polarizable continuum model (PCM-TDDFT). In addition to vibrational frequency, proton NMR is also assigned for the respective vibrations and nuclear resonance peaks for comparison with the available experimental values. Comparison of the experimental spectra with calculated excitation and emission energy, including solvent effect, provides a high accuracy among the results obtained for NP. The results obtained are promising and demonstrated the versatility of this chromophore, and the combined use of continuum solvation methods, and experimental spectroscopic data can indeed represent a step towards more extensive application in research fields of current interests.

**Acknowledgments** Authors S.S.M. and S.R. thank UGC for providing SRF. Author S.C. thanks CSIR for providing SRF. We are thankful to S. Sarkar for his kind cooperation.

## References

1. Ferreira R, Remón P, Pischel U (2009) Multivalued logic with a tristable fluorescent switch. J Phys Chem C 113:5805–5811
2. Banerjee S, Veale EB, Phelan CM, Murphy SA, Tocci GM, Gillespie LJ, Frimannsson DO, Kelly JM, Gunnlaugsson T (2013) Recent advances in the development of 1,8-naphthalimide based DNA targeting binders, anticancer and fluorescent cellular imaging agents. Chem Soc Rev 42:1601–1618
3. Manna A, Chakravorti S (2010) Charge transfer in 1,8-Naphthalimide: a combined theoretical and experimental approach. Photochem Photobiol 86:47–54
4. Coronado JLG, Martín E, Montero LA, Fierro JLG, García de la Vega JM (2007) Effects of the 3- and 4-Methoxy and Acetamide substituents and solvent environment on the electronic properties of N-substituted 1,8-Naphthalimide derivatives. J Phys Chem A 111: 9724–9732

5. Qi Q, Ha Y, Sun Y (2010) Density functional studies of the substituent effect on absorption and emission properties of 1, 8-naphthalimide derivatives. J Mol Model 16:1179–1186
6. Wei S, Sun Y, Guo P, Hu X, Fan J (2012) A novel 4-(tetrahydro-2-furanmethoxy)-*N*-octadecyl-1,8-naphthalimide based blue emitting probe: solvent effect on the photophysical properties and protein detection. Russ J Bioorg Chem 38:469–478
7. k-Nagy KS, Biczók L (2004) Effect of protonation and hydrogen bonding on the fluorescent properties and exciplex formation of *N*-(4-pyridyl)-1,2-naphthalimide. Photochem Photobiol Sci 3:389–395
8. Miao L, Yao Y, Yang F, Wanga Z, Li W, Hub J (2008) A TDDFT and PCM-TDDFT studies on absorption spectra of N-substituted 1,8-naphthalimides dyes. J Mol Struct THEOCHEM 865:79–87
9. Jin R, Tang S (2013) Theoretical investigation into optical and electronic properties of 1,8-naphthalimide derivatives. J Mol Model 19: 1685–1693
10. Yang R, Guo X, Wang W, Zhang Y, Jia L (2012) Highly selective and sensitive chemosensor for $Hg^{2+}$ based on the naphthalimide fluorophore. J Fluoresc 22:1065–1071
11. Brana MF, Ramos A (2001) Naphthalimides as anti-cancer agents: synthesis and biological activity. Curr Med Chem 1:237–255
12. Kucheryavy P, Li G, Vyas S, Hadad C, Glusac KD (2009) Electronic properties of 4-substituted naphthalimides. J Phys Chem A 113: 6453–6461
13. Bran MF, Gradillas A, Gomez A, Acero N, Llinares F, Munoz-Mingarro D, Abradelo C, Rey-Stolle F, Yuste M, Campos J, Gallo MA, Espinosa A (2004) Synthesis, biological activity, and quantitative structure-activity relationship study of Azanaphthalimide and Arylnaphthalimide derivatives. J Med Chem 47:2236–2242
14. Georgiev NI, Bojinov VB, Venkova AI (2013) Design, synthesis and ph sensing properties of novel pamam light-harvesting dendrons based on rhodamine 6 g and 1,8-naphthalimide. J Fluoresc 23:459–471
15. Niu CG, Qin PZ, Zeng GM, Gui XQ, Guan AL (2007) Fluorescence sensor for water in organic solvents prepared from covalent immobilization of 4-morpholinyl-1, 8-naphthalimide. Anal Bioanal Chem 387:1067–1074
16. Chatterjee S, Pramanik S, Hossain SU, Bhattacharya S, Bhattacharya SC (2007) Synthesis and photoinduced intramolecular charge transfer of *N*-substituted 1,8-naphthalimide derivatives in homogeneous solvents and in presence of reduced glutathione. J Photochem Photobiol A 187:64–71
17. Singha Roy S, Ghosh P, Hossain SU, Chakraborty P, Biswas J, Mandal S, Bhattacharya A, Bhattacharya S (2010) Naphthalimide based novel organoselenocyanates: Finding less toxic forms of selenium that would retain protective efficacy. Bioorg Med Chem Lett 20:6951–6955
18. Casida ME (1995) In: Chong DP (ed) Recent advances in density functional methods. Part I. World Scientific, Singapore
19. Gross EKU, Dobson JF, Petersilka M (1996) In: Nalewajski RF (ed) Density functional theory II. Springer, Heidelberg
20. Nithya R, Santhanamoorthi N, Kolandaivel P, Senthilkumar K (2011) Structural and spectral properties of 4-Bromo-1-naphthyl chalcones: a quantum chemical study. J Phys Chem A 115:6594–6602
21. Li W, Wang YB, Pavel I, Yuan Q, Ye Y, Fu EQ, Luo MD, Hu JM, Kiefer W (2005) DFT/TDDFT studies of the geometry, electronic structure and spectra of (12S)-1,4,7,10-tetraazadicyclo[10,3,0]-pentadecane-3,11-dione and its derivatives. J Phys Chem A 109: 2878–2886
22. Vogel AI (1994) Textbook of practical organic chemistry, 5th edn. Singapore Publishers Ltd, Singapore, pp 397–403
23. Sarkar A, Mandal TK, Rana DK, Dhar S, Chall S, Bhattacharya SC (2010) Tuning the photophysics of a bio-active molecular probe '3-pyrazolyl-2-pyrazoline' derivative in different solvents: dual effect of polarity and hydrogen bonding. J Lumin 130:2271–2276
24. Hohenberg P, Kohn W (1964) Inhomogeneous electron gas. Phys Rev 136:B864–B871
25. Kohn W, Sham LJ (1965) Self-consistent equations including exchange and correlation effects. Phys Rev 140:A1133–A1138
26. Becke AD (1993) Density-functional thermochemistry. III. The role of exact exchange. J Chem Phys 98:5648–5652
27. Lee CT, Yang WT, Parr RG (1988) Development of the Colle-Salvetti correlation-energy formula into a functional of the electron density. Phys Rev B 37:785–789
28. Saranya G, Kolandaivel P, Senthilkumar K (2011) Optical absorption and emission properties of fluoranthene, benzo[k]fluoranthene, and their derivatives. A DFT study. J Phys Chem A 115:14647–14656
29. Arulmozhiraja S, Ehara M, Nakatsuji HJ (2008) Electronic transitions in *cis*- and *trans*-dichloroethylenes and tetrachloroethylene. J Chem Phys 129:174506
30. Qi Q, Ha Y, Sun Y (2011) Structural and solvent effects on the spectroscopic properties of 1, 8-naphthalimide derivatives: a density functional study. Int J Quantum Chem 111:2234–2241
31. Li N, Jia K, Wang S, Xia A (2007) Theoretical study of spectroscopic properties of dimethoxy-p-phenylene-ethynylene oligomers: planarization of the conjugated backbone. J Phys Chem A 111: 9393–9398
32. Navarro FC, Mitnik DG (2012) DFT study of the effect of substituents on the absorption and emission spectra of Indigo. Chem Cent J 6(70):1–6
33. Stratmann RE, Scuseria GE, Frisch MJ (1998) An efficient implementation of time-dependent density-functional theory for the calculation of excitation energies of large molecules. J Chem Phys 109: 8218–8224
34. Casida ME, Jamorski C, Casida KC, Salahub DR (1998) Molecular excitation energies to high-lying bound states from timedependent density-functional response theory: characterization and correction of the time-dependent local density approximation ionization threshold. J Chem Phys 108:4439–4449
35. Barone V, Cossi M, Tomasi J (1998) Geometry optimization of molecular structures in solution by the polarizable continuum model. J Comput Chem 19:404–417
36. Frisch MJ, Trucks GW, Schlegel HB, Scuseria GE, Robb MA, Cheeseman RJ, Montgomery JJA, Vreven T, Kudin KN, Burant JC, Millam JM, Iyengar SS, Tomasi J, Barone V, Mennucci B, Cossi M, Scalmani G, Rega N, Petersson GA, Nakatsuji H, Hada M, Ehara M, Toyota K, Fukuda R, Hasegawa J, Ishida M, Nakajima T, Honda Y, Kitao O, Nakai H, Klene M, Li X, Knox JE, Hratchian HP, Cross JB, Adamo C, Jaramillo J, Gomperts R, Stratmann RE, Yazyev O, Austin AJ, Cammi R, Pomelli C, Ochterski JW, Ayala PY, Morokuma K, Voth GA, Salvador P, Dannenberg JJ, Zakrzewski VG, Dapprich S, Daniels AD, Strain MC, Farkas O, Malick DK, Rabuck AD, Raghavachari K, Foresman JB, Ortiz JV, Cui Q, Baboul AG, Clifford S, Cioslowski J, Stefanov BB, Liu G, Liashenko A, Piskorz P, Komaromi I, Martin RL, Fox DJ, Keith T, Al-Laham MA, Peng CY, Nanayakkara A, Challacombe M, Gill PMW, Johnson B, Chen W, Wong MW, Gonzalez C, Pople JA (2004) Gaussian 03, Revision E.01. Gaussian, Inc, Wallingford
37. Reichardt C (1988) Solvents and solvent effects in organic chemistry, 2nd edn. VCH, Weinheim
38. Dimroth K, Reichardt C, Siepmann T, Bohlmann F (1963) Über pyridinium-*N*-phenol-betaine und ihre Verwendung zur Charakterisierung der Polarität von Lösungsmitteln. Justus Liebigs Ann Chem 661:1–37
39. Dhar S, Singha Roy S, Rana DK, Bhattacharya S, Bhattacharya S, Bhattacharya SC (2011) Tunable solvatochromic response of newly synthesized antioxidative naphthalimide derivatives: intramolecular charge transfer associated with hydrogen bonding effect. J Phys Chem A 115:2216–2224

40. Dey J, Warner IM (1997) Dual fluorescence of 9-(N, N-Dimethylamino)anthracene: effect of solvent polarity and viscosity. J Phys Chem A 101:4872–4878
41. Ye JY, Yamauchi M, Yogi O, Ishikawa M (1999) Spectroscopic Properties of 2′-(or-3′)-*O*-(2,4,6-trinitrophenyl) adenosine 5′-Triphosphate revealed by time-resolved fluorescence spectroscopy. J Phys Chem B 103:2812–2817
42. Kamlet MJ, Abboud JLM, Abraham MH, Taft RW (1983) Linear solvation energy relationships. 23. A comprehensive collection of the solvatochromic parameters, $\pi^*$, $\alpha$, and $\beta$, and some methods for simplifying the generalized solvatochromic equation. J Org Chem 48:2877–2887
43. Abraham MH, Greillier PL, Abboud JLM, Doherty RM, Taft RW (1988) Solvent effects in organic chemistry - recent developments. Can J Chem 66:2673–2686
44. Mati SS, Sarkar S, Sarkar P, Bhattacharya SC (2012) Explicit spectral response of the geometrical isomers of a bio-active pyrazoline derivative encapsulated in β-cyclodextrin nanocavity: a photophysical and quantum chemical analysis. J Phys Chem A 116:10371–10382
45. Dhar S, Rana DK, Singha Roy S, Roy S, Bhattacharya S, Bhattacharya SC (2012) Effect of solvent environment on the photophysics of a newly synthesized bioactive 7-oxy(5-selenocyanato-pentyl)-2*H*-1-benzopyran-2-one. J Lumin 132:957–964
46. Gan J, Chen K, Chang C, Tian H (2003) Luminescent properties and photo-induced electron transfer of naphthalimides with piperazine substituent. Dyes Pigments 57:21–28
47. Poteau X, Brown AI, Brown RG, Holmes C, Matthew D (2000) Fluorescence switching in 4-amino-1,8-naphthalimides: "on–off–on" operation controlled by solvent and cations. Dyes Pigments 47: 91–105
48. Pradhan T, Ghoshal P, Biswas R (2008) Structural transition in alcohol-water binary mixtures: a spectroscopic study. J Chem Sci 120:275–287
49. Sarkar A, Banerjee P, Hossain SU, Bhattacharya S, Bhattacharya SC (2009) Role of hydrogen bonding on the spectroscopic properties of thiazolidinedione derivatives in homogeneous solvents. Spectrochim Acta A 72:1097–1102
50. Mennucci B, Caricato M, Ingrosso F, Cappelli C, Cammi R, Tomasi J, Scalmani G, Frisch MJ (2008) How the environment controls absorption and fluorescence spectra of PRODAN: a quantum-mechanical study in homogeneous and heterogeneous media. J Phys Chem B 112:414–423
51. Dodoff NI (2012) A DFT/ECP-small basis set modelling of cisplatin: molecular structure and vibrational spectrum. Comput Mol Biosci 2: 35–44
52. Yakhanthip T, Kungwan N, Jitonnom J, Anuragudom P, Jungsuttiwong S, Hannongbua S (2011) Theoretical investigation on the electronic and optical properties of poly(fluorenevinylene) derivatives as light-emitting materials. Int J Photoenergy 570103:1–9
53. Grabchev I, Bojinov V, Petkov C (2003) Infrared absorption studies of some new 1,8-naphthalimide. Chem Heterocycl Compd 39:179–183